Molecular Cloning, Cell-surface displayed expression of VHH against VEGF Expressed in E. coli by ice nucleation protein (INP)

المعبر عنه في VEGF ضد VHH الاستنساخ الجزيئي، التعبير المعروض على سطح الخلية عن E. coli بواسطة بروتين نواة الجليد (INP)

Salim Alhafyan
Corresponding: saleembio89@gmail.com
Submitted Date: 6 May 2024 - Accepted Date: 24 June 2024

ABSTRACT

Angiogenesis plays a crucial role in various physiological and pathological processes, including tumor growth, where VEGF is considered the most critical factor in this process. Nowadays, the production of single-domain antibodies (VHH) with the ability to inhibit growth factors in cancer tumors is emerging as a novel approach in cancer therapy. In our previous research, it was identified that camelid VHHs generated through phage display against VEGF play a significant role in the inhibition of VEGF. Among these VHHs, the one with the highest affinity for the VEGF receptor was selected from the phage display VHH library. Considering the efficiency of surface expression in E. coli using the ice nucleation protein (INP) anchoring motif, this system was employed for protein expression. Given that only the C-terminal domain of the INP is involved in cell surface attachment, a gene structure of 537 bp starting from the InaK gene was utilized in the design. Surface expression was performed using the pET-21a containing INP and VEvhh10 against VEGF. The results indicated that the INP sequence is a suitable option for surface expression of VEvhh10 in E. coli. After the production of unbound VEvhh10, isolation, and purification by centrifugation and multiple washes were carried out, followed by examination of its binding to VEGF. The successful binding of VEvhh10 to VEGF demonstrates that the resulting non-fused protein could be utilized for future therapeutic and clinical diagnostic applications in patients.
Keywords: Bacterial Surface Display, Ice Nucleation Protein, Vhh, Angiogenesis, Vascular Endothelial Growth Factor

الملخص

يلعب تكوين الأوعية دوراً حاسماً في كثير من العمليات الفسيولوجية والمرضية، بما في ذلك نمو الورم، حيث يُعدُّ VEGF العامل الأكثر أهمية في هذه العمليات. في الوقت الحاضر، يبرز إنتاج الأجسام المضادة أحادية المجال (VHH) القادرة على تثبيط عوامل النمو في الأورام السرطانية بوصفه نهجاً جديداً في علاج السرطان. في بحثنا السابق، تم اكتشاف أن VHHs ضد VEGF المولدة بوساطة عرض العاثيات تلعب دوراً مهماً في تثبيط VEGF. من بين هذه الـ VHHs، جرى اختيار النوع الذي يتمتع بأعلى درجة تقارب لمستقبل VEGF من مكتبة VHH التي عُرضت بوساطة العاثيات. وبالنظر إلى كفاءة التعبير السطحي في الإشريكية القولونية باستخدام نموذج بروتين نواة الجليد (INP)، فقد استُخدم هذا النظام للتعبير عن البروتين. ونظراً لأن مجال C–terminal الخاص بـ INP هو فقط المشارك في الارتباط بسطح الخلية، فقد استُخدمت بنية جينية تبلغ ٥٣٧ نوكليوتيداً من بداية جين InaK. أُجري التعبير السطحي باستخدام pET–a٢١ الذي يحتوي على INP و VEvhh١٠ ضد VEGF. أشارت النتائج إلى أن تسلسل INP يعد خياراً مناسباً للتعبير السطحي عن VEvhh١٠ في E. coli. بعد إنتاج VEvhh١٠ غير المرتبط، أُجريت عمليات العزل والتنقية باستخدام الطرد المركزي والغسلات المتعددة، وتلاها فحص ارتباطه بـ VEGF. يوضح الارتباط الناجح لـ VEvhh١٠ بـ VEGF أن البروتين غير المدمج الناتج يمكن استخدامه في التطبيقات التشخيصية العلاجية والسريرية المستقبلية لدى المرضى.

INTRODUCTION

Vascular Endothelial Growth Factor (VEGF) is a homodimeric glycoprotein with a molecular weight of approximately 28 KD. This protein serves as a critical mediator for angiogenesis, the formation of new blood vessels. VEGF exerts its physiological effects by binding to two receptors known as Flt-1 (VEGFR-I) and KDR (VEGFR-II) (1). These receptors possess seven

extracellular immunoglobulin-like domains and one intracellular tyrosine kinase domain. They are expressed on the surface of endothelial cells, playing a critical role in the regulation of angiogenesis (3 ,2). Under hypoxic conditions, the expression of VEGF receptors increases, leading to the induction of the angiogenesis phenomenon. The binding of VEGF to the VEGFR-II receptor stimulates the response of endothelial cells in blood vessels (6-4). Although VEGFR-I has a higher affinity for this factor, it only plays a role in sequestering VEGF and facilitates its access to the VEGFR-II receptor, which is the primary receptor mediating antigenic signaling. VEGF binds to these receptors through two distinct domains (8 ,7). In healthy individuals, VEGF contributes to angiogenesis during embryonic development and plays a critical role in adult wound healing. Pathological angiogenesis is pivotal in various conditions such as tumor growth, metastasis, diabetic retinopathy, macular degeneration, rheumatoid arthritis, and psoriasis (11-9). Inhibition of angiogenesis can be achieved by several methods, including inhibition of endothelial cell signal transduction, migration, and survival, as well as modulation of factors such as growth, proliferation, matrix metalloproteinase, and bone marrow precursor cells. VEGF, as a regulator of tumor angiogenesis, exerts its angiogenic effects by binding to its receptors, especially VEGFR-II, thereby influencing the mentioned processes (14-12). Therefore, this molecule is of great importance as a valuable drug target in antiangiogenic therapies (15 ,12). In this study, to overcome this issue, a surface display technique was chosen, allowing peptides to be presented on the surface of microbial cells through fusion with anchoring motifs. The ice nucleation protein (INP) is one of the joint membrane proteins in bacteria (27-22). Despite the size limitations that most surface expression systems have regarding the display of target proteins on the cell surface, an INP-based surface expression system can express and display VHH on the bacterial surface, and overcoming the problems of cytoplasmic expression within bacteria.

MATERIALS AND METHODS

Molecular and Chemical Materials

The materials, chemicals, and reagents required for the lab are listed as follows:
·Ampicillin and Agarose from Acros (Taiwan)
·IPTG from SinaClon (Iran)
·Ni-NTA resin from Qiagen (Netherlands)
·Plasmid extraction kit and gel extraction kit from GeneAll (South Korea)
·Enzyme purification kit from Yektatajhiz (Iran)
·Restriction enzymes HindIII/XhoI, ligase enzyme, and other molecular enzymes from Fermentas (USA).
·pfu polymerase and Taq polymerase from Vivantis (South Korea)
·Primers from Sinagen (Iran)
·Methylthiazole-tetrazolium (MTT) powder from Sigma (USA)
·Penicillin-Streptomycin, Trypsin-EDTA, and DMED-low glucose from Bio-Idea (Iran)
·Fetal Bovine Serum (FBS) from GibcoBRL (USA)
·A monoclonal conjugated anti-human antibody with HRP from Pishgaman Teb (Iran)
·Anti-Austen antibody from Roche (Switzerland)

Design of fusion genes and constructions of pET-INP-VHH

Gene Cloning: Primers for the amplification of the VEvhh10 gene with the accession code LC010469 were initially designed (Table 1). The plasmid containing the gene fragment served as a template for the Polymerase Chain Reaction (PCR). Amplification was carried out using Taq polymerase and Pfu polymerase enzymes in a thermocycler with a programmed temperature profile (Table 2). Various annealing temperatures for primer binding to the template were tested, and a temperature of 65°C was found to be the optimal annealing temperature. Primer cutting sites at the beginning and end of the Gene were designed, and the location of the TEV protease enzyme cutting site was positioned between the INP linker and the VEvhh10 sequence.

Table 1: Primer Sequences for Amplification of the VEvhh$_{10}$ Gene with Accession Code LC010469

	Sequence'5'→'3'	Tm (°C)
Forward primer	**CCCAAGCTTGAGAATCTATATTTTCAGGGCCAGGTGCAGCTGCAGGAGTC**	**69.7**
Reverse primer	**CCGCTCGAGCTATGAGGAGACGGTGAYCTGGGTC**	**68.3**

The VEvhh10 gene fragment, amplified by the pfu polymerase through PCR, was extracted from the gel. Simultaneously, digestion of this fragment and the pET-21a vector containing the INP linker was carried out using the HindIII and XhoI restriction enzymes. Purification was performed using a commercial enzyme purification kit. Ligation of the gene fragment into the target vector was accomplished using the T4 DNA ligase enzyme. The resulting product was incubated at 4°C overnight. The ligated product was then transferred into E. coli DH-5α bacteria. To confirm the Gene insertion into the vector, the transformed bacteria were plated on antibiotic- ampicillin containing plates. The obtained colonies were then subjected to Colony PCR using specific primers for VHH, T7 promoter, and terminator primers. The PCR products were analyzed on a %1 agarose gel, and positive transformants were screened and cultured. The recombinant plasmid was purified using a plasmid extraction kit. Enzymatic dual digestion by HindIII and XhoI was performed to confirm the insertion of the gene fragment into the plasmid.

Table 2: Thermal Cycling Conditions for Colony PCR in this Study

Steps	Reaction	*Taq* polymerase		*Pfu*	
		Temperature °C	Time	Temperature °C	Time
1	Initial denaturation	95	6 min	95	5 min
2	Denaturation	95	30 Sec	95	30 Sec
3	Annealing	64-51	30 Sec	61-67	30 Sec
4	Extension	72	1 min	72	2 min

Expression and detection of the Gene constructs InaK-N_TEV Protease

The gene structure of the InaK-N_TEV Protease was transformed in the pET-21a plasmid containing INP and VHH using a heat shock method in the E. coli BL21 (DE3) host. For protein expression, a colony from bacteria harboring the recombinant plasmid was inoculated into 10 mL LB medium supplemented with 100 mg/ml ampicillin and incubated at 37 °C with adequate aeration (250 rpm). Subsequently, 1 mL of the grown bacteria was transferred to 50 mL LB medium containing ampicillin and incubated at 37 °C until the OD600 reached approximately 0.6. Finally, expression was induced with 1 mM IPTG for 24 hours at 25 °C. The resulting product was centrifuged at 4000 rpm for 15 minutes, and the obtained pellet was stored at -20 °C until further analysis. To confirm protein expression, SDS-PAGE (Sodium Dodecyl Sulfate-Polyacrylamide Gel Electrophoresis) was performed using a %12 acrylamide gel under non-reducing conditions according to the Laemmli method (28).

The expression and purification of VEGF109-8

The pET-28a plasmid containing the VEGF109-8 gene (the domain binding to the VEGF receptor) was transformed into E. coli BL21 (DE3) bacterial cells and cultured at 37 °C overnight in Terrific Broth (TB) medium supplemented with 100 mg/ml kanamycin. Subsequently, induction was carried out with 0.5 mM IPTG at an OD600 of 0.6, and the cells were incubated at 24 °C for 22 hours (29). After centrifugation (5000 g, 15 minutes, 4 °C), the bacterial cells were sonicated in a lysis buffer containing 50 mM NaH2PO300 ,4 mM NaCl, 10 mM imidazole, and 1 mM PMSF (pH 8.0). The sonication product was further centrifuged at 12000 rpm for 20 minutes at 4 °C. The resulting supernatant was analyzed using SDS-PAGE for further characterization (30). Protein purification was carried out using affinity chromatography with a nickel column. For this purpose, the protein sample was transferred onto a column that had previously reached equilibrium by washing with a wash buffer (Tris-base (50 mM, pH 8.0) + NaCl (300 mM) + Imidazole (20 mM)). At this stage, proteins lacking a histidine tag were washed out and removed from the column using this buffer. Only the target protein, due to the presence of a histidine tag, remained bound to the column. Subsequently, using the elution buffer (Tris-base (50 mM, pH 8.0) + NaCl (300 mM) + Imidazole (250 mM)) in the presence of a high concentration of imidazole, protein separation was performed. Additionally, purification was conducted using cold buffers to prevent the thermal denaturation of proteins. Following that, dialysis was performed in PBS buffer containing glycerol overnight at 4 °C, and the protein was analyzed using SDS-PAGE. Protein concentration was determined by the Bradford method with BSA as a protein standard (31).

Cell Culture

Human Umbilical Vein Endothelial Cells (HUVEC) were cultured in T25 flasks using Dulbecco's Modified Eagle Medium (DMEM) supplemented with 5 mM glucose, 2 mM L-glutamine, %10 fetal bovine serum (FBS), %1 penicillin (100 mg/mL), and streptomycin (100 mg/mL). The

cells were maintained at 37°C with %5 CO2 and used for subsequent experiments (32).

In vitro endothelial cell proliferation assay

In order to investigate the effect of VEGF109-8 on the growth and proliferation of HUVECs, the MTT colorimetric method was employed (33). A total of 103×5 cells were seeded in each well of a 96-well culture plate. After cell attachment within 24 hours, the culture medium was replaced with fresh medium containing VEGF109-8-RBD protein at various concentrations (120 ,60 ,30 ,10, and 240 ng /mL), and the cells were incubated at 37 °C for 48 hours. Three independent assessments were performed for each treatment. For cell proliferation determination, cells were treated with 0.5 mg/mL MTT for 4 hours at 37 °C, and then the medium was carefully removed. Formazan crystals were dissolved in 100 µL of DMSO, and the absorbance was read at 570 nm using a µQuant plate reader from BioTek (USA).

ELISA-based immunoassay

The surface-expressed VHH-expressing bacterial cells, using the INP anchor, were prepared in a carbonate-bicarbonate buffer (pH 0.1 ,9.6 M Na2CO0.1 ,3 M NaHCO3). Subsequently, 100 µL of bacterial cells containing the INP-VEvhh10 linker were added to each well and incubated at room temperature for 16 hours. After 16 hours, the solution was aspirated, and the wells were washed three times with 100 µL of PBS buffer. Blocking was performed using a blocking buffer consisting of %2 gelatin in PBS (350 µL) for one hour at 37 °C. The blocking solution was then aspirated, and the wells were washed three times with 100 µL of PBST buffer (PBS + %0.05 Tween-20). Serial dilutions of VEGF solutions (ranging from 5.0 ng/ mL to 500 ng/mL) were added to the wells and incubated for 2 hours at room temperature. After incubation, all wells were aspirated and washed thoroughly with PBST buffer. Subsequently, 100 µL of human monoclonal anti-VEGF antibody at a concentration of 1000 ng/mL was added to each well, followed by incubation in the dark at 37 °C for 1.5 hours. Then, 100 µL of Anti-Human IgG conjugated with HRP were added to each well and incubated in the dark at 37 °C for 1.5 hours. Finally, 100 µL of TMB and H2O2 were added to each well and incubated for 15 minutes in the dark. The reaction was stopped by adding 100 µL of 2 N sulfuric acid to each well. The absorbance of the wells was then read at 450 nm wavelength.

RESULTS

Construction of pET-21a-Ina_K537-TEV-VEvhh10 expression plasmid

A schematic representation of the gene structure pET-21a-Ina_K537-TEV-VEvhh10 is presented in (Figure 1) using Snapgene.v5.1.5 software. Initially, the plasmid pComb3X containing the VEvhh10 gene sequence with the accession number LC010469 in the GenBank database was registered and extracted from E. coli TG bacteria using the Gene All kit. Subsequently, the plasmid served as a template for VEvhh10 gene amplification using specific primers for the VEvhh10 gene (414bp), Taq DNA polymerase (Figure 2a), and pfu polymerase (Figure 2b). After the amplification process, the PCR product (VEvhh10) was digested with HindIII and XhoI enzymes to create cohesive ends, It has been cleaned (402bp) (Figure 2c). Additionally, the pET-21a vector containing the INP linker was linearized through digestion with HindIII and XhoI restriction enzymes for subsequent pure attachment, the results of this stage were as expected in terms of nucleotide sequence counts. After ligation, the resulting product (pET-21a-Ina -TEV-VEvhh10) was incubated at 4 for 14 h and then introduced into bacteria. The transformed product was cultured on ampicillin-containing LB plates. Positive samples were isolated and confirmed for gene insertion using colony PCR. Subsequently, the extracted pET-21a-Ina_K537-TEV-VEvhh10 plasmid was used as a template for amplifying the VEvhh10 gene and the gene structure containing INP. The PCR was performed on the plasmid extraction using Forward and Reverse primers for the VEvhh10 gene 414bp as shown (Figure 3a) and, likewise, Forward and Reverse primers for the T7 promoter and terminator of the plasmid 1099bp as shown (Figure 3b). The plasmid was digested with HindIII and XhoI enzymes, resulting in the visualization of the target gene on the gel (Figure 3c). After examination, the results indicated the success and confirmation of the cloning.

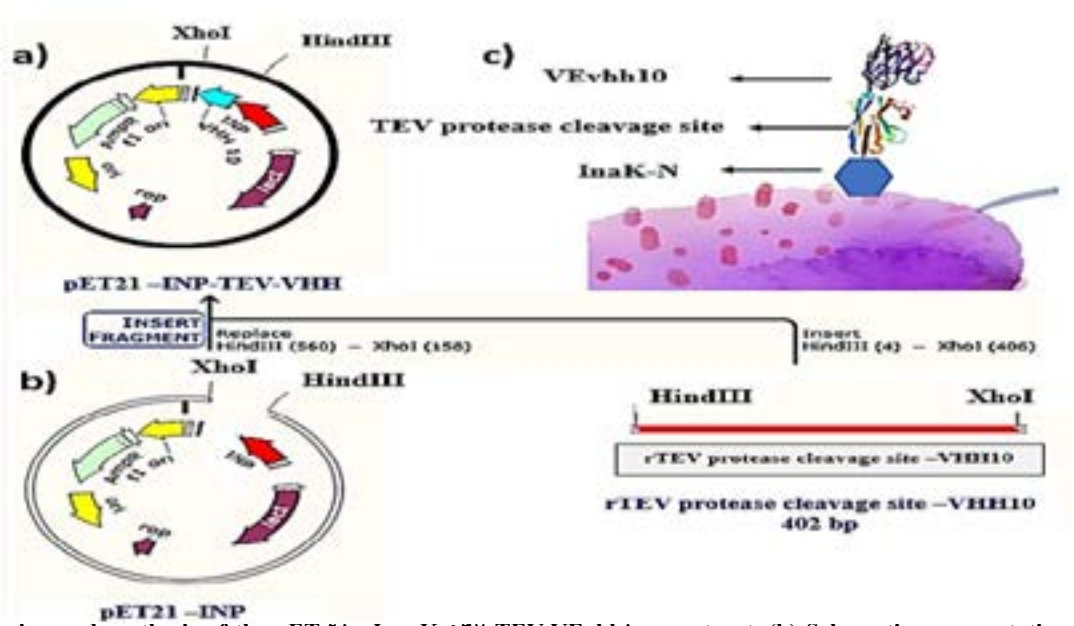

Figure ١: (a) Design and synthesis of the pET-٢١a-Ina_K ٥٣٧-TEV-VEvhh١٠ construct. (b) Schematic representation of the pET-٢١a plasmid containing Ina_K ٥٣٧, linearly designed according to cuts with HindIII and XhoI enzymes. The final product (TEV-VEvhh١٠) from PCR, with an added site for TEV protease enzyme cleavage before the VEvhh١٠ sequence, resulted in a length of ٤٠٢ bp. (c) Schematic representation of the surface expression of VEvhh١٠ using the ice nucleation protein in the E. coli host.

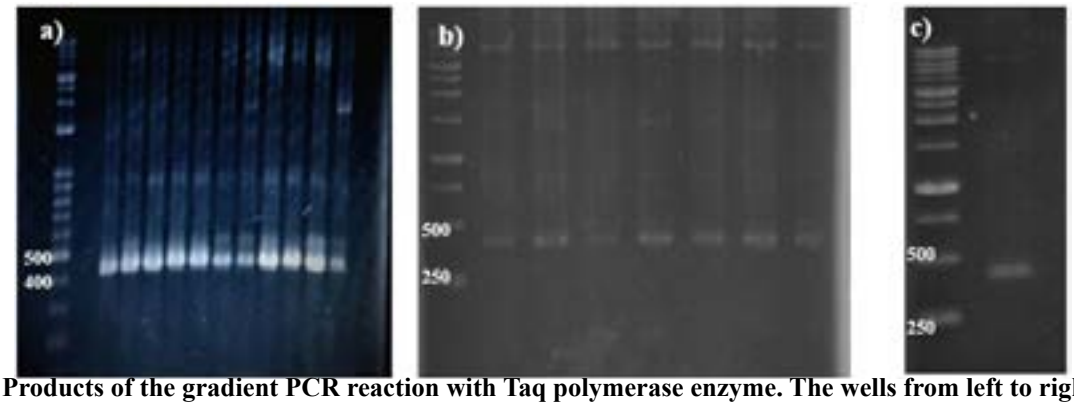

Figure ٢: (a) Products of the gradient PCR reaction with Taq polymerase enzyme. The wells from left to right include DNA ladder PCR products for annealing temperatures of °C ٥٢,٢ ,٥٣,٥ ,٥٥ ,٥٧,٥ ,٥٨ ,٥٩,٦ ,٦١,١ ,٦٢,٩ ,٦٤,٤, and ٥١. (b) PCR gradient with pfu polymerase enzyme. The wells from left to right include a DNA ladder, annealing temperatures ranging from °C ٦١ to °C ٦٧. (c) PCR products with pfu enzyme after dual digestion and purification

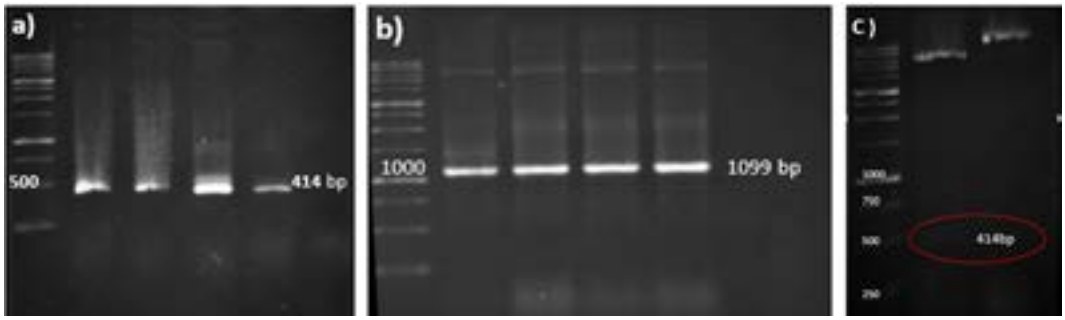

Figure ٣: Examination of plasmids with specific primers for VHH (a) and primers for the T٧ promoter and T٧ terminator (b) obtained from different extractions. (c) Confirmation of the VHH gene ligation process into the pET-٢١a plasmid containing INP, from left to right: DNA ladder, double digestion of the plasmid with enzymes (HindIII, XhoI), and positive control sample containing undigested plasmid.

Confirmation of Surface Expression Ina_K537-TEV-VEvhh10

The InaK-N_TEV Protease_Cleavage_Site_ VEvhh10 structure consists of three parts: the initial 537 bp of the InaK gene from Pseudomonas syringae encoding a protein with an approximate molecular weight of 19-KD, the VEvhh10 mono body gene with 372 bp and a protein with an approximate molecular weight of 14 KD, and the coding sequence for the TEV protease cleavage site with 21bp. Therefore, the molecular weight of the unmodified InaK-N_TEV Protease_ Cleavage_Site_VEvhh10 structure is around 33 KD. To investigate the surface expression of VHH, bacterial pellets were divided into three parts after expression. The first part underwent sonication, the second part was digested with lysozyme, and the third part remained as intact cells (Figure 4).

Each of these fractions was also treated with the TEV protease, and the results obtained in SDS-PAGE non-denaturing gel are shown (Figure 4). The appearance of a band in the 33-KD range in SDS-PAGE for the lysed bacterial pellet induced with IPTG, in comparison to the control sample, indicates the expression of this protein. Bands in lanes 3 ,1, and 5 represent the expressed surface protein in the presence of TEV protease, indicating a weak TEV protease band and an additional 19-KD band corresponding to INP. In contrast, lanes 4 ,2, and 6 show bands corresponding to the expressed surface protein in the absence of TEV protease, and these bands are stronger compared to the previous condition. Additionally, due to the lack of cleavage by TEV protease, the band corresponding to INP did not appear. These results indicate the successful surface expression of VEvhh10 (Figure 5).

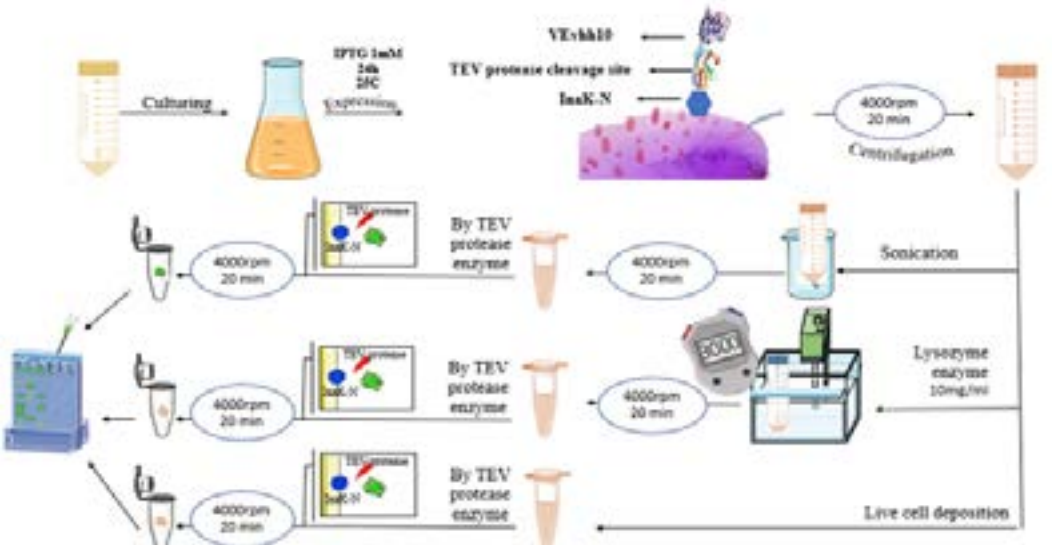

Figure ٤: General schematic of the process that was conducted to investigate the surface display of EVvhh١٠ in E. coli bacteria.

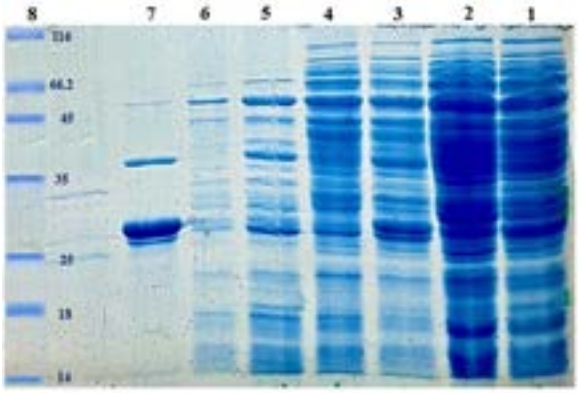

Figure ٥: Columns (٣ ,١, and ٥) contain live cell pellet, sonicated, and lysed samples with the presence of protease enzyme; samples in columns (٤ ,٢, and ٦) include live cell pellet, sonicated, and lysed without protease enzyme, column ٧ (TEV protease), and column ٨ protein marker.

In vitro HUVECs proliferation assay

Before investigating the binding capability of the expressed VHH on the bacterial surface, the activity of the produced non-fused VEGF109-8 was assessed by its effect on the growth and proliferation of human umbilical vein endothelial cells (HUVECs) using the MTT assay. As illustrated in Figure 6, cell proliferation is well-performed with an increase in the concentration of non-fused VEGF109-8. At a concentration of 240 ng/mL, the cell population has reached approximately %80 compared to the sample lacking VEGF109-8. Therefore, the produced non-fused VEGF exhibits biological activity and can be utilized in VHH binding assays.

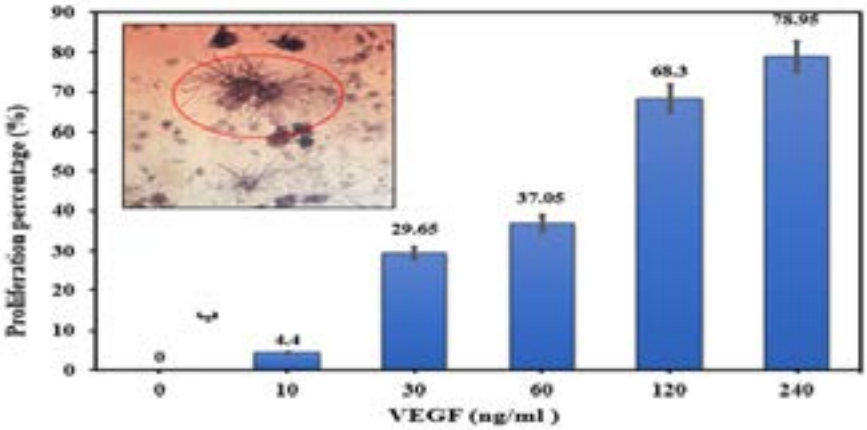

Figure 6: The effect of recombinant VEGF109-8 concentration on the growth of umbilical vein endothelial cells (HUVECs) in different concentrations. As the concentration of VEGF109-8 non-fused increases, cell growth shows a dose-dependent response, reaching optimal proliferation at a concentration of 240 ng/mL.

Evaluation of binding of VHHs of VEGF

In order to assess the binding capability of VEvhh10 to VEGF, an ELISA-based immune assay was employed following the mentioned method (Figure 7a). The results obtained from the dose-response curve of VEvhh10 expressed on the bacterial surface using the ELISA method (Figure 7b) demonstrated that an increase in VEGF concentration led to a higher number of anti-VEGF molecules binding to it, resulting in an enhanced optical absorption.

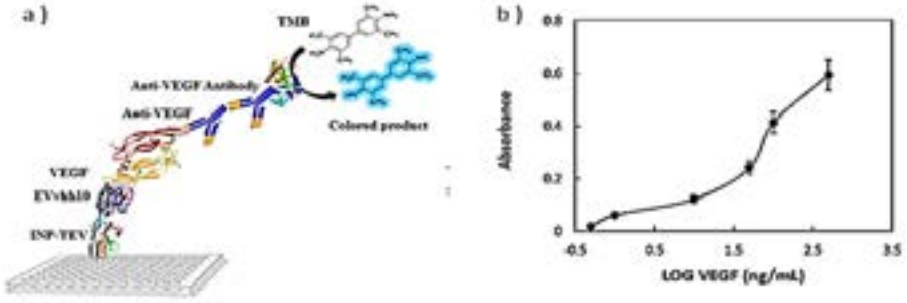

Figure ٧: a) Schematic representation of the ELISA-based immune assay for measuring VEGF concentration using surface-displayed EVvhh١٠ on bacterial cells. b) Dose-response curve of surface-expressed EVvhh١٠ in ELISA for VEGF detection.

DISCUSSION

According to global statistics, cancer is one of the problems that the world community is facing (34). One promising approach is to inhibit angiogenesis, the formation of new blood vessels, which tumors rely on for growth. Tumor cells can undergo cell death due to oxygen and nutrient deficiency if new vascular systems do not develop. However, when the vascular system extends towards the tumor, it can continue growing. Since angiogenesis is a common requirement across many cancers, targeting it is an effective strategy for tumor elimination. Tumor cells promote vascular growth by secreting VEGF, which affects endothelial cells, triggers signaling cascades, and increases cell proliferation, migration, and survival (36 ,35). Vascular endothelial growth factor (VEGF) is the key inducer of angiogenesis, which is crucial for tumor growth and metastasis. Under pathological conditions, VEGF expression significantly increases, with %60 of cancer cells upregulating VEGF to facilitate growth. VEGF promotes endothelial cell proliferation and migration, and increases vascular permeability and protease expression, aiding angiogenesis (10). Due to its pivotal role, VEGF is a primary therapeutic target. Inhibiting VEGF involves strategies like monoclonal antibodies, VEGF mutants, receptor antagonists, soluble receptors, tyrosine kinase inhibitors, anti-sense methods, and aptamers. VEGF functions by binding to its tyrosine kinase receptors (VEGFR-I and VEGFR-II), leading to receptor dimerization and phosphorylation (5). In recent years, targeted therapy using monoclonal antibodies has gained significant attention and emerged as one of the most successful strategies for treating hematologic malignancies and solid tumors. Monoclonal antibodies eliminate tumor cells through various mechanisms, including

direct impacts on tumor cells (e.g., blocking receptors), immune system-mediated cell-killing, and specific impacts on tumor angiogenesis (37). While monoclonal antibodies have shown promise in targeted cancer therapy (17 ,16), they also come with drawbacks like immunogenicity, high production costs, and limited tumor tissue penetration due to their large size. Effective cancer treatment requires specific properties in monoclonal antibodies, including specificity, solubility, stability, and smaller size. Efforts have focused on producing antibody fragments like scFV and Fab, which offer advantages such as enhanced tumor penetration, reduced immunogenicity, and faster production. However, challenges remain in terms of stability, expression yield, aggregation, and protease resistance, necessitating further improvements (38). In the camelid family, unique immunoglobulins lacking light chains are found in the mammalian immune system. These heavy-chain antibodies feature a VHH domain, which maintains antigen-binding ability akin to full antibodies while overcoming the challenges of conventional antibodies and engineered fragments. Their exceptional characteristics include high stability and solubility, ease of production, small size, heat, detergent, and protease resistance, high homology with human VHH fragments, high antigen affinity, ease of humanization, and engineering into multi-specific forms. Due to their small size, VHHs are expected to penetrate tumors and the retina more effectively than other antibodies. Moreover, VHHs are the only option among antibodies and their derivatives capable of crossing the blood-brain barrier. Therefore, VHHs with VEGF inhibition potential hold promise for angiogenesis inhibition in brain tumors as well (40 ,39). Given the extraordinary importance of angiogenesis inhibition in cancer and other diseases, the remarkable success of monoclonal antibodies against VEGF in this field and the superiority of VHHs over other antibodies and antigen-binding fragments have been established. In this study, a surface display system using the INP linker was employed to produce VHH antibodies with high specificity and affinity against VEGF in the bacterial system. The use of a surface display system has various advantages, including low cost, easy expression, and ease of control over expression conditions (41). In this study, we employed a surface display system using the INP linker to produce VHH antibodies targeting VEGF in bacteria, addressing the challenges associated with bacterial cytoplasmic expression (40). The INP-based system offers advantages such as low cost, easy expression, and control over expression conditions. Additionally, the central repetitive region in INP can be removed to produce shorter fusion proteins for cell surface display (42). Despite size limitations in some systems, INP allows expression of proteins up to 60 kD. Various variants of INP exist, with Ina-K being the most commonly used (43), so in this study, the N-terminal region of InaK, which contains the first 537 amino acid pairs of Ina-K, was employed as an anchor motif for displaying VEvhh10 on the surface of bacterial cells. In a 2015 study, Shahangian et al. designed and constructed phages displaying single-domain antibodies targeting the region linked to the VEGF receptor. These phages exhibited binding capability to key functional regions. A phage display library on a nanobody platform was prepared, followed by enrichment and competitive screening of VHHs targeting VEGFR-II using competitive ELISA. Monoclonal VHHs with the highest affinity for the second binding domain of the VEGF receptor were sequenced and named VEvhh1, VEvhh2, and VEvhh3 (VEvhh10) based on their recurrence frequency. The gene sequences encoding these VHHs are deposited in GenBank with accession numbers LC010467, LC010468, and LC010469, respectively(19). The results of this research indicate that the use of the surface display system with the INP linker for expressing VEvhh10 is a suitable option. This system completely eliminates the need for cell lysis and time-consuming, costly chromatographic methods. With this system, it is possible to express VEvhh10 as shown (Figure 5). Furthermore, the ELISA results and the cell proliferation assay (live-cell assay) confirm that VEvhh10 binds with high affinity to the VEGF receptor binding region, as shown in the (Figure 7.b). Ultimately, a previously unexplored INP, InaA, was successfully used to display VEvhh10 on the cell surface of E. coli BL21 (DE3) (Figure 1.c). The InaK-N_TEV Protease_Cleavage_Site_ VEvhh10 detected on SDS-PAGE was 33 kD, exactly as expected. The expression of VEvhh10 on the bacterial cell surface was verified using the INP Linker. An immunological examination was conducted using an ELISA-based immune assay to measure VEGF concentration in the presence of different VEGF concentrations. As indicated in (Figure 7.b), the results demonstrated

that increasing VEGF concentration led to a higher number of anti-VEGF molecules binding (VEvhh10 expressed on the bacterial cell surface), resulting in enhanced optical absorption. This study shows that it is possible to overcome the problems of cytoplasmic expression in bacteria by using a surface expression system. This system transfers VEvhh10 to be expressed on the bacterial cell surface using a linker INP, thus overcoming the problem of incorrect folding inside the bacteria. The information obtained from this study introduces VEvhh10 as a suitable candidate for inhibiting VEGF. It has the capability to block the key functional site of VEGF, inhibiting its binding to its receptor and consequently preventing the cascade of its signaling. However, further studies and investigations are required to validate this proposal.

ACKNOWLEDGMENT

The Researcher expresses sincere gratitude to the Research Deputy of Tarbiat Modares University for providing laboratory facilities and financial support.

REFERENCES

1. Ferrara N. Molecular Basis of Angiogenesis and its Application. The Keio Journal of Medicine. 2024;73(1):12-.
2. Chandler KB, Leon DR, Meyer RD, Rahimi N, Costello CE. Site-specific N-glycosylation of endothelial cell receptor tyrosine kinase VEGFR-2. Journal of proteome research. 2017;16(2):677-88.
3. Melincovici CS, Boşca AB, Şuşman S, Mărginean M, Mihu C, Istrate M, et al. Vascular endothelial growth factor (VEGF)-key factor in normal and pathological angiogenesis. Rom J Morphol Embryol. 2018;59(2):455-67.
4. Mariotti V, Fiorotto R, Cadamuro M, Fabris L, Strazzabosco M. New insights on the role of vascular endothelial growth factor in biliary pathophysiology. JHEP Reports. 2021;3(3):100251.
5. Lange C, Storkebaum E, De Almodóvar CR, Dewerchin M, Carmeliet P. Vascular endothelial growth factor: a neurovascular target in neurological diseases. Nature Reviews Neurology. 2016;12(8):439-54.
6. Wang X, Bove AM, Simone G, Ma B. Molecular bases of VEGFR-2-mediated physiological function and pathological role. Frontiers in Cell and Developmental Biology. 2020;8:599281.
7. Keyt BA, Nguyen HV, Berleau LT, Duarte CM, Park J, Chen H, Ferrara N. Identification of Vascular Endothelial Growth Factor Determinants for Binding KDR and FLT-1 Receptors: GENERATION OF RECEPTOR-SELECTIVE VEGF VARIANTS BY SITE-DIRECTED MUTAGENESIS ( ). Journal of Biological Chemistry. 1996;271(10):5638-46.
8. Wiesmann C, Fuh G, Christinger HW, Eigenbrot C, Wells JA, de Vos AM. Crystal structure at 1.7 Å resolution of VEGF in complex with domain 2 of the Flt-1 receptor. Cell. 1997;91(5):695-704.
9. Kelly AG, Panigrahy D. Targeting angiogenesis via resolution of inflammation. Cold Spring Harbor Perspectives in Medicine. 2023;13(3):a041172.
10. Ghavamipour F, Shahangian SS, Sajedi RH, Arab SS, Mansouri K, Aghamaali MR. Development of a highly-potent anti-angiogenic VEGF 8–109 heterodimer by directed blocking of its VEGFR-2 binding site. The FEBS journal. 2014;281(19):4479-94.
11. Caplan ES, Kesselheim AS. Anti-VEGF therapy in ophthalmology: a qualitative analysis of transformative drug development. Drug discovery today. 2016;21(6):1019-26.
12. Pathak A, Pal AK, Roy S, Nandave M, Jain K. Role of Angiogenesis and Its Biomarkers in Development of Targeted Tumor Therapies. Stem Cells International. 2024;2024.
13. Al Kawas H, Saaid I, Jank P, Westhoff CC, Denkert C, Pross T, et al. How VEGF-A and its splice variants affect breast cancer development–clinical implications. Cellular Oncology. 2022;45(2):227-39.
14. Zhang M, Liu J, Liu G, Xing Z, Jia Z, Li J, et al. Anti-vascular endothelial growth factor therapy in breast cancer: Molecular pathway, potential targets, and current treatment strategies. Cancer Letters. 2021;520:422-33.
15. Li AQ, Fang JH. Anti-angiogenic therapy enhances cancer immunotherapy: Mechanism and clinical application. Interdisciplinary Medicine. 2024;2(1):e20230025.
16. Deschacht N, De Groeve K, Vincke C, Raes G, De Baetselier P, Muyldermans S. A novel promiscuous class of camelid single-domain antibody contributes to the antigen-binding repertoire. The Journal of Immunology. 2010;184(10):5696-704.
17. Cortez-Retamozo V, Backmann N, Senter PD, Wernery U, De Baetselier P, Muyldermans S, Revets H. Efficient cancer therapy with a nanobody-based conjugate. Cancer research. 2004;64(8):2853-7.
18. Zhang Q, Zhang N, Xiao H, Wang C, He L. Small Antibodies with Big Applications: Nanobody-Based Cancer Diagnostics and Therapeutics. Cancers. 2023;15(23):5639.
19. Shahangian SS, Sajedi RH, Hasannia S, Jalili S, Mohammadi M, Taghdir M, et al. A conformation-based phage-display panning to screen neutralizing anti-VEGF VHHs with VEGFR2 mimicry behavior. International journal of biological macromolecules. 2015;77:222-34.
20. Bu D, Zhou Y, Tang J, Jing F, Zhang W. Expression and purification of a novel therapeutic single-chain variable fragment antibody against BNP from inclusion bodies of Escherichia coli. Protein expression and purification. 2013;92(2):203-7.
21. Yuasa N, Koyama T, Fujita-Yamaguchi Y. Purification and refolding of anti-T-antigen single chain antibodies (scFvs) expressed in Escherichia coli as inclusion bodies. BioScience Trends. 2014;8(1):24-31.
22. Jeong J, Selvamani V, Maruthamuthu Mk, Arulsamy K, Hong SH. Application of the surface engineered recombinant Escherichia coli to the industrial battery waste solution for lithium recovery. Journal of Industrial Microbiology and Biotechnology. 2024;51:kuae012.
23. Vázquez-Arias A, Vázquez-Iglesias L, Pérez-Juste I, Pérez-Juste J, Pastoriza-Santos I, Bodelon G. Bacterial surface display of human lectins in Escherichia coli. Microbial Biotechnology. 2024:e14409.
24. Downey ML, Peralta-Yahya P. Technologies for the discovery of G protein–coupled receptor–targeting biologics. Current Opinion in Biotechnology. 2024;87:103138.
25. Ali J, Faridi S, Kashyap A, Noori R, Sardar M. Surface expression of carbonic anhydrase on E. coli as a sustainable approach for enzymatic CO2 capture. Enzyme and Microbial Technology. 2024:110422.
26. Park M. Surface display technology for biosensor applications: a review. Sensors. 2020;20(10):2775.
27. Wang Y, Wang Q, Shan X, Wu Y, Hou S, Zhang A, Hou Y. Characteristics of cold-adapted carbonic anhydrase and

efficient carbon dioxide capture based on cell surface display technology. Bioresource Technology. 2024;399:130539.
28. Laemmli UK. Cleavage of structural proteins during the assembly of the head of bacteriophage T4. nature. 1970;227(5259):680-5.
29. Rezaei S, Takalloo Z, Rezaei ZS, Babaeipour V, Talebi AF, Sajedi RH. Soluble overexpression, high-level production and purification of receptor binding domain of human VEGF8-109 in E. coli. Process Biochemistry. 2020;96:228-38.
30. Ramakrishnan S, Sulochana K, Punitham R, Arunagiri K. Free alanine, aspartic acid, or glutamic acid reduce the glycation of human lens proteins. Glycoconjugate journal. 1996;13(4):519-23.
31. Bradford N. A rapid and sensitive method for the quantitation microgram quantities of a protein isolated from red cell membranes. Anal Biochem. 1976;72(248):e254.
32. Kamiloglu S, Sari G, Ozdal T, Capanoglu E. Guidelines for cell viability assays. Food Frontiers. 2020;1(3):332-49.
33. Wang Q, Zeng A, Zhu M, Song L. Dual inhibition of EGFR-VEGF: An effective approach to the treatment of advanced non-small cell lung cancer with EGFR mutation. International journal of oncology. 2023;62(2):1-10.
34. Klein C, Brinkmann U, Reichert JM, Kontermann RE. The present and future of bispecific antibodies for cancer therapy. Nature Reviews Drug Discovery. 2024:1-19.
35. Morgos D-T, Stefani C, Miricescu D, Greabu M, Stanciu S, Nica S, et al. Targeting PI3K/AKT/mTOR and MAPK Signaling Pathways in Gastric Cancer. International Journal of Molecular Sciences. 2024;25(3):1848.
36. Shaw P, Dwivedi SKD, Bhattacharya R, Mukherjee P, Rao G. VEGF signaling: Role in angiogenesis and beyond. Biochimica et Biophysica Acta (BBA)-Reviews on Cancer. 2024:189079.
37. Scott AM, Wolchok JD, Old LJ. Antibody therapy of cancer. Nature reviews cancer. 2012;12(4):278-87.
38. Quintero-Hernández V, Juárez-González VR, Ortíz-León M, Sánchez R, Possani LD, Becerril B. The change of the scFv into the Fab format improves the stability and in vivo toxin neutralization capacity of recombinant antibodies. Molecular immunology. 2007;44(6):1307-15.
39. Cong Y, Devoogdt N, Lambin P, Dubois LJ, Yaromina A. Promising Diagnostic and Therapeutic Approaches Based on VHHs for Cancer Management. Cancers. 2024;16(2):371.
40. Kumar GV, Manicum A-LE, Makwikwi T, Chakafana G, Agwamba EC, Katerere DR. Functionalized nanobody-based delivery systems for cancer diagnosis and therapeutic applications. Functionalized Nanomaterials for Cancer Research: Elsevier; 2024. p. 283-305.
41. Narang AS, Mahato RI. Targeted delivery of small and macromolecular drugs: CRC press; 2010.
42. Bao S, Yu S, Guo X, Zhang F, Sun Y, Tan L, et al. Construction of a cell-surface display system based on the N-terminal domain of ice nucleation protein and its application in identification of mycoplasma adhesion proteins. Journal of applied microbiology. 2015;119(1):236-44.
43. Kotrba P. Microbial biosorption of metals—general introduction. Microbial biosorption of metals: Springer; 2011. p. 1-6.

Fund: No fund

Author Contributions: All the work made by the author.

Competing interests: The Authors declare that they have no competing interests.

Data and materials availability: All data are available in the main text.